2007-01-2490

A ROBUST FORMULATION FOR PREDICTION OF HUMAN RUNNING

Hyun-Joon Chung, Yujiang Xiang, Anith Mathai, Salam Rahmatalla, Joo Kim, Timothy Marler, Steve Beck, Jingzhou Yang, Jasbir Arora, Karim Abdel-Malek
Virtual Soldier Research Program, Center for Computer Aided Design, The University of Iowa, Iowa City, IA 52242, USA

John Obusek
U.S. Army Soldier Center, Natick, MA 01760, USA

ABSTRACT

A method to simulate digital human running using an optimization-based approach is presented. The digital human is considered as a mechanical system that includes link lengths, mass moments of inertia, joint torques, and external forces. The problem is formulated as an optimization problem to determine the joint angle profiles. The kinematics analysis of the model is carried out using the Denavit-Hartenberg method. The B-spline approximation is used for discretization of the joint angle profiles, and the recursive formulation is used for the dynamic equilibrium analysis. The equations of motion thus obtained are treated as equality constraints in the optimization process. With this formulation, a method for the integration of constrained equations of motion is not required. This is a unique feature of the present formulation and has advantages for the numerical solution process. The formulation also offers considerable flexibility for simulating different running conditions quite routinely. The zero moment point (ZMP) constraint during the foot support phase is imposed in the optimization problem. The proposed approach works quite well, and several realistic simulations of human running are generated.

INTRODUCTION

The 3D digital human running problem is formulated as an optimization-based predictive dynamics problem. It is noted that the expression “predictive dynamics” has been coined to characterize a class of physics-based problems that are modeled using differential equations of motion and that would otherwise require the solution of such problems using time-step integration. However, in this case, predictive dynamics is a broadly applicable formulation for addressing such problems using optimization techniques without having to integrate the equations of motion. Indeed, the formulation does not have a unique solution, and constraints play an important role in the solution process.

In the problem of running, the objective is to predict (or calculate) joint angles and torques at the joints over time, also called joint and torque profiles, respectively. For the problem of running, a minimal set of constraints is imposed in the formulation of the problem to simulate natural running of the digital human. The human running problem is distinguished from the walking problem in that there is a flight phase during each step of running. In the present formulation, running steps are assumed to be periodic and symmetric for the right and left steps. Both the support phase and the flight phase are modeled. A companion paper by Xiang, et al (2007) presents the formulation for the human walking problem.

The digital human is modeled as a mechanical system that includes link lengths, mass moments of inertia, joint torques, and external forces. The entire model has 55 degrees of freedom (DOF)—6 for global translation and rotation and 49 for the body. A DOF in this case characterizes a kinematics jointed pair in the kinematics sense, where various segments of the body are assumed to be connected by revolute joints. The B-spline interpolation is used for time discretization, and the Denavit-Hartenberg (DH) method is used for kinematics analysis. The recursive Lagrangian formulation is used for the equations of motion; it was chosen because it is considered to be quite efficient. The equations of motion are verified by the forward dynamics process using a commercial general-purpose multi-body dynamics software code.

The problem is formulated as a nonlinear optimization problem. A unique feature of the formulation is that the equations of motion are not integrated explicitly; this has become the most important contribution because it provides for a generalized method to solve dynamic indeterminate problems that would otherwise require computationally intensive integration methods. They are imposed as equality constraints in the optimization process. An algorithm based on the sequential quadratic programming approach is used to solve the nonlinear optimization problem. The control points for the joint

Report Documentation Page

Form Approved
OMB No. 0704-0188

1. REPORT DATE	2. REPORT TYPE	3. DATES COVERED
JUN 2007		**00-00-2007 to 00-00-2007**

4. TITLE AND SUBTITLE	5a. CONTRACT NUMBER
A Robust Formulation for Prediction of Human Running	5b. GRANT NUMBER
	5c. PROGRAM ELEMENT NUMBER
6. AUTHOR(S)	5d. PROJECT NUMBER
	5e. TASK NUMBER
	5f. WORK UNIT NUMBER
7. PERFORMING ORGANIZATION NAME(S) AND ADDRESS(ES) **University of Iowa,Center for Computer Aided Design ,Vrtual Sodier Research Program,Iowa City,IA,52242**	8. PERFORMING ORGANIZATION REPORT NUMBER
9. SPONSORING/MONITORING AGENCY NAME(S) AND ADDRESS(ES)	10. SPONSOR/MONITOR'S ACRONYM(S)
	11. SPONSOR/MONITOR'S REPORT NUMBER(S)

12. DISTRIBUTION/AVAILABILITY STATEMENT
Approved for public release; distribution unlimited

13. SUPPLEMENTARY NOTES
SAE Digital Human Modeling Conference, June 2007, Seattle, WA, Society of Automotive Engineers, Warrendale, PA.

14. ABSTRACT
A method to simulate digital human running using an optimization-based approach is presented. The digital human is considered as a mechanical system that includes link lengths, mass moments of inertia, joint torques, and external forces. The problem is formulated as an optimization problem to determine the joint angle profiles. The kinematics analysis of the model is carried out using the Denavit-Hartenberg method. The B-spline approximation is used for discretization of the joint angle profiles, and the recursive formulation is used for the dynamic equilibrium analysis. The equations of motion thus obtained are treated as equality constraints in the optimization process. With this formulation, a method for the integration of constrained equations of motion is not required. This is a unique feature of the present formulation and has advantages for the numerical solution process. The formulation also offers considerable flexibility for simulating different running conditions quite routinely. The zero moment point (ZMP) constraint during the foot support phase is imposed in the optimization problem. The proposed approach works quite well, and several realistic simulations of human running are generated.

15. SUBJECT TERMS

16. SECURITY CLASSIFICATION OF:			17. LIMITATION OF ABSTRACT	18. NUMBER OF PAGES	19a. NAME OF RESPONSIBLE PERSON
a. REPORT **unclassified**	b. ABSTRACT **unclassified**	c. THIS PAGE **unclassified**	**Same as Report (SAR)**	**11**	

angle profiles are treated as design variables; when calculated, they provide for the complete motion. For the performance measure in the optimization problem, the mechanical energy that is represented as the integral of the sum of the squares of all the joint torques is minimized. The dynamic stability is achieved by satisfying the zero moment point (ZMP) constraint in the support phase. The zero yawing moment (ZYM) constraint is imposed so that the upper-body motion is compensated by the lower-body motion. The solution is simulated in the Santos™ human modeling and simulation environment. The simulations show a very natural running motion of the digital human. The joint torque and angle profiles and ground reaction forces are recovered from the simulation. A couple of simulations of running at different speeds and carrying loads on the back are generated quite routinely and efficiently.

Virtual human dynamics simulation is a very active area of research. In recent years, many papers have been published on biped digital human motion. For the digital human running problem, however, there are only a few papers in the robotics area. In the biomechanics area, reports have been mostly on experimental research involving subjects rather than the dynamics simulation of the problem.

Biomechanics: Cavanagh and Lafortune (1980) studied ground reaction forces and center of pressure (COP) patterns for 18 subjects during running. Simpson and Bates (1990) experimented with the effect of running speed on joint moments in the support phase. Ounpuu (1994) described the terminology, kinematics, and kinetics of human walking and running in clinics in a sports medicine journal. Novacheck (1998) summarized the biomechanics of human running. He discussed kinematics, kinetics, COP, and muscle activities in relation to EMG results and injuries.

Robotics: Many researchers have worked on the problem of walking robots. Since walking and running are considered part of biped locomotion, there are many papers in the robotics walking area that are relevant for the running problem. For example, the zero moment point (ZMP) dynamics stability constraint (Vukobratović et al., 1990) can be included in the running problem as well as the walking problem. However, only the literature about the running problem will be discussed in this section. Honda has been developing humanoid robots since 1986, and their robot Advanced Step in Innovative Mobility (ASIMO) is the most advanced running robot to date. ASIMO can run at 6 km/h. Fujimoto (2004) used an optimization technique for creating trajectory for a biped running robot. The idea was to minimize energy consumption due to the biped robot's running motion by determining the joint angles and torques. This work was done for a 2D model that had only 7 DOF. Nagasaki et al. (2003) generated the running pattern by using the angular momentum and the control theory; however, only a few seconds of simulation was performed. Roussel et al. (1998) published about the generation of an energy-optimal complete gait for biped robots. This work did not discuss the running problem, but it included an impulse term in the cost function, which will be considered in the running problem in the present study. Park and Kwon (2003) developed a biped robot's running motion by using the impedance control. Hybrid Zero Dynamics (HZD) was presented by Westervelt and Grizzle (2003). The robot walked with quite a natural motion with that method, but it did not have 3D stability.

Computer Graphics: Basically, the methods to generate locomotion in robotics and animation are similar. However, animators are more interested in high-level behavior, while researchers in robotics are interested in joint torques and forces. Hodgins (1996) simulated 3D digital human running. The approach basically used the control theory for the mechanical system, and commercial software was used for the dynamics solution of the mechanical system. However, 3D stability was not considered in her work. Kang et al. (1999) proposed a model based on a one-legged planar hopper with a self-balancing mechanism for human running animation.

In previous work, Kim et al. (2004) developed an optimization-based dynamic motion prediction method for the digital human gait. They used B-spline, the DH method, and ZMP/ZYM stability for the walking problem. However, the joint torques could not be obtained with that formulation because the equations of motion were not considered. Currently, the equations of motion and their sensitivities are included so that the joint torques can be obtained.

Considering the human running gait cycle, the running style depends on the speed of running. For example, at slower running speeds, the heel touches the ground first. In fast running or sprinting, the fore-foot touches the ground first. Moreover, the upper body motion is different for slower and faster running (sprinting). The faster the runner's speed, the more arm swinging motion is generated to minimize energy consumption. Running is differentiated from walking not by the speed but by the existence of a flight phase. During a walk, whether slow or fast, there exists a double support phase (where both feet are on the ground). The period from the initial contact of one foot to the following contact of the same foot is called the *gait cycle*. One gait cycle of running is composed of two phases: the support phase and the flight phase. The flight phase starts with a toe off and ends with the strike of the other foot. The support phase starts with a foot strike and ends with same foot's toe off (Figure 1). In the area of biomechanics, the distance from one foot's strike to the other foot's strike is called a *step*. Also, the distance from one foot's strike to the same foot's subsequent strike is called a *stride*.

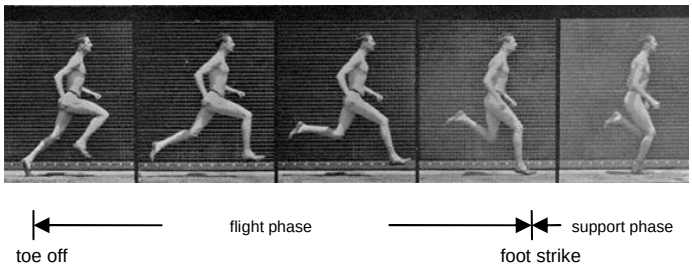

Figure 1 Human running cycle (Photo by Edward Muybridge)

OPTIMIZTION –BASED PREDICTIVE DYNAMICS

Using optimization techniques, the digital human's motion can be predicted as along with the relative joint torques and external forces. The basic idea is to determine joint angle profiles and torque profiles to optimize some objective function (for example, metabolic energy consumption and joint torques). Figure 2 explains the entire optimization process. First, the initial control point values for the joint angle profiles are given. Then, the control points are passed on to the analysis module. The analysis module uses the B-spline module, DH module, equations of motion module, and cost function/constraints module. Through this module, cost function and constraints values are obtained. Using the cost function and constraint functions values and their gradients, the optimization module checks whether or not the current values are optimum. The SNOPT program is used for the optimization module. If the stopping criteria are not satisfied, the B-spline control points are updated by the optimization module. The entire process is repeated again until an optimum solution is obtained. The B-spline method, DH method, and equations of motion are discussed in the next section.

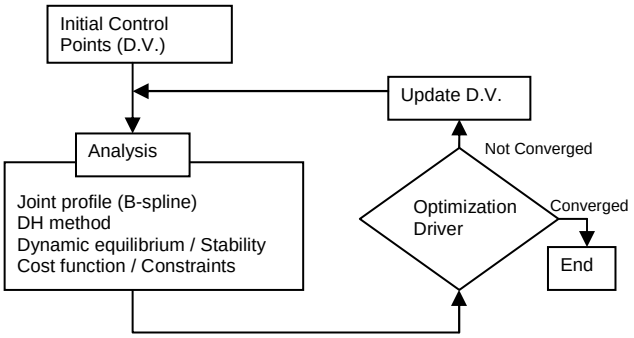

Figure 2 Optimization-based Predictive Dynamics Process

JOINT ANGLE PROFILE APPROXIMATION

B-SPLINE APPROXIMATION

The joint angles are functions of time. These functions can be represented as a linear combination of cubic B-spline basis functions. Given a knot vector $\mathbf{t} = \{t_0, t_1, t_2,..., t_m\}$ and control points $\hat{q}_0\ \hat{q}_1\ \hat{q}_2\ ,..., \hat{q}_n$, the approximation is defined as

$$q(t) = \sum_{i=0}^{n} N_{i,p}(t)\hat{q}_i \tag{1}$$

where $N_{i,p}$ is the i^{th} basis function of degree p. The basis function $N_{i,p}(t)$ is given in the recursive form as

$$N_{i,p}(t,\mathbf{t}) = \left(\frac{t-t_i}{t_{i+p}-t_i}\right)N_{i,p-1}(t,\mathbf{t}) + \left(\frac{t_{i+p+1}-t}{t_{i+p+1}-t_{i+1}}\right)N_{i+1,p-1}(t,\mathbf{t}) \tag{2}$$

and

$$N_{i,0}(t,\mathbf{t}) = \begin{cases} 1 & (t_i \le t < t_{i+1}) \\ 0 & \text{otherwise} \end{cases} \tag{3}$$

The relation between the number of knots m+1 and the number of control points n+1 is

$$m = n + p + 1 \tag{4}$$

CUBIC B-SPLINE CURVES

The Cubic B-spline curves which have basis functions of degree 3 in the local interval $t_i \le t < t_{i+1}$ is

$$q(t) = \sum_{j=0}^{3} N_{i-j,3}(t)\hat{q}_{i-j} \qquad i \ge 3 \tag{5}$$

and

$$N_{i-3,3} = \frac{(t_{i+1}-t)^3}{(t_{i+1}-t_i)(t_{i+1}-t_{i-1})(t_{i+1}-t_{i-2})} \tag{6a}$$

$$N_{i-2,3} = \frac{(t-t_{i-2})(t_{i+1}-t)^2}{(t_{i+1}-t_{i-2})(t_{i+1}-t_{i-1})(t_{i+2}-t_i)} + \frac{(t-t_{i-1})(t_{i+1}-t)(t_{i+2}-t)}{(t_{i+1}-t_{i-1})(t_{i+1}-t_i)(t_{i+2}-t_{i-1})} + \frac{(t-t_i)(t_{i+2}-t)^2}{(t_{i+1}-t_i)(t_{i+2}-t_{i-1})(t_{i+2}-t_i)} \tag{6b}$$

$$N_{i-1,3} = \frac{(t-t_{i-1})^2(t_{i+1}-t)}{(t_{i+1}-t_{i-1})(t_{i+1}-t_i)(t_{i+2}-t_{i-1})} + \frac{(t-t_{i-1})(t-t_i)(t_{i+2}-t)}{(t_{i+1}-t_i)(t_{i+2}-t_{i-1})(t_{i+2}-t_i)} + \frac{(t-t_i)^2(t_{i+3}-t)}{(t_{i+1}-t_i)(t_{i+2}-t_i)(t_{i+3}-t_i)} \tag{6c}$$

$$N_{i,3} = \frac{(t-t_i)^3}{(t_{i+1}-t_i)(t_{i+2}-t_i)(t_{i+3}-t_i)} \tag{6d}$$

To generate clamped B-spline curves which touch the first and last control points, multiple knots of multiplicity 4 are used at the first and the last knots.

KINEMATIC MODEL OF HUMAN BODY

DENAVIT-HARTENBERG METHOD

Denavit and Hartenberg (1955) proposed a matrix transformation method to describe the translational and rotational relationship systematically between adjacent links in articulated chain. This matrix transformation representation is called the DH method. The transformation matrix is a 4×4 homogeneous matrix. This method represents each link coordinate system in terms of the previous link coordinate system. Then any local coordinate system (including the end-effector of the manipulator or serial chain) can be expressed in an original reference by the DH method. Basically, the method represents a vector in one coordinate frame in terms of the other coordinate frame. This method has its base in the field of robotics but can be used for modeling human kinematics as well.

Consider articulated chains, which are depicted in Figure 3.

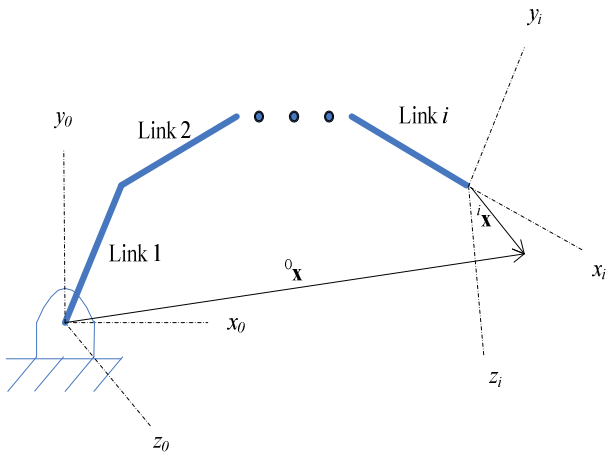

Figure 3 Articulated chains

Any point of interest in the i^{th} frame ${}^i\mathbf{x}$ can be transferred to the global reference frame ${}^0\mathbf{x}$:

$$ {}^0\mathbf{x} = {}^0\mathbf{T}_i \, {}^i\mathbf{x} \tag{7} $$

where ${}^i\mathbf{x}$ is a 4×1 vector in terms of the i^{th} reference frame and ${}^0\mathbf{T}_i$ is a 4×4 homogeneous transformation matrix from the i^{th} reference frame to the global reference frame.

Here the transformation of a vector to the global reference frame is simply multiplication of transformation matrices, which is given as:

$$ {}^0\mathbf{T}_i = {}^0\mathbf{T}_1 \, {}^1\mathbf{T}_2 \cdots {}^{i-1}\mathbf{T}_i = \prod_{n=1}^{i} {}^{n-1}\mathbf{T}_n \tag{8} $$

The transformation matrix of this vector is a 4×4 matrix that includes 4 DH parameters, which are described in Figure 4.

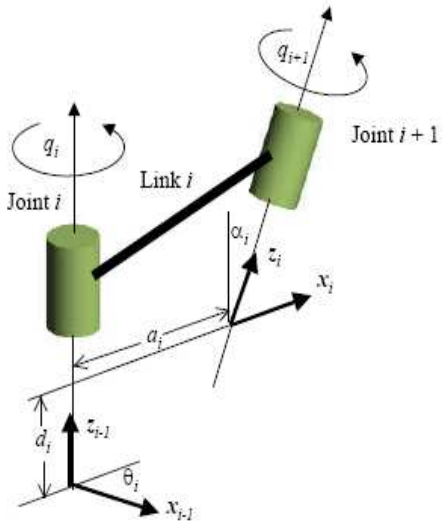

Figure 4 DH parameters

DH parameters in Figure 4 are defined as follows:

- θ_i is the joint angle between the $\mathbf{x}_{i-1}$ axis and the $\mathbf{x}_i$ axis about the $\mathbf{z}_{i-1}$ axis according to the right-hand rule.
- d_i is the distance between the origin of the $i-1^{\text{th}}$ coordinate frame and the intersection of the $\mathbf{z}_{i-1}$ axis with the $\mathbf{x}_i$ axis along the $\mathbf{z}_{i-1}$ axis.
- a_i is the distance between the intersection of the $\mathbf{z}_{i-1}$ axis with the $\mathbf{x}_i$ axis and the origin of the i^{th} frame along the $\mathbf{x}_i$ axis. Or, the shortest distance between the $\mathbf{z}_{i-1}$ and $\mathbf{z}_i$ axes.
- α_i is the angle between the $\mathbf{z}_{i-1}$ axis and the $\mathbf{z}_i$ axis about the $\mathbf{x}_i$ axis according to the right-hand rule.

Then, the DH transformation matrix from i^{th} frame to $i-1^{\text{th}}$ frame is written as:

$$ {}^{i-1}\mathbf{T}_i = \begin{bmatrix} \cos\theta_i & -\cos\alpha_i \sin\theta_i & \sin\alpha_i \sin\theta_i & a_i \cos\theta_i \\ \sin\theta_i & \cos\alpha_i \cos\theta_i & -\sin\alpha_i \cos\theta_i & a_i \sin\theta_i \\ 0 & \sin\alpha_i & \cos\alpha_i & d_i \\ 0 & 0 & 0 & 1 \end{bmatrix} \tag{9} $$

Among the four DH parameters, the rotation about the z axis is treated as the rotational DOF in the mechanical model, and the other three parameters are fixed. Therefore, each transformation has one DOF. The current Santos™ model has 55 DOF, including 6 global DOF. The global DOF are composed of three translations and three rotations. A full-body digital human model is depicted in Figure 5. Note that spine, neck, shoulder and hip joint have 3 rotational DOF.

Elbow, clavicle, ankle and wrist joint have 2 rotational DOF. Knee and toe joint have 1 rotational DOF.

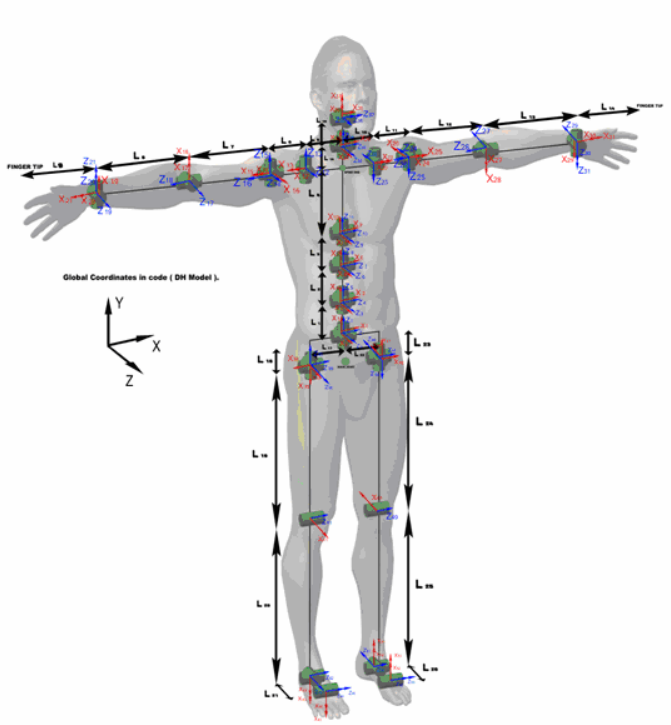

Figure 5 Mechanical structure of Santos based on DH method

KINEMATIC ANALYSIS OF HUMAN BODY

The kinematics analysis in the recursive form leads to a simpler form for the transformation matrix $\mathbf{A}_i$ Time derivatives of the transformation matrix $\mathbf{A}_i$ can be obtained in the recursive form as:

$$\mathbf{A}_i = \mathbf{A}_{i-1}\mathbf{T}_i \tag{10a}$$

$$\mathbf{B}_i = \dot{\mathbf{A}}_i = \mathbf{B}_{i-1}\mathbf{T}_i + \mathbf{A}_{i-1}\frac{\partial \mathbf{T}_i}{\partial q_i}\dot{q}_i \tag{10b}$$

$$\mathbf{C}_i = \dot{\mathbf{B}}_i = \mathbf{C}_{i-1}\mathbf{T}_i + 2\mathbf{B}_{i-1}\frac{\partial \mathbf{T}_i}{\partial q_i}\dot{q}_i + \mathbf{A}_{i-1}\frac{\partial^2 \mathbf{T}_i}{\partial q_i^2}\dot{q}_i^2 + \mathbf{A}_{i-1}\frac{\partial \mathbf{T}_i}{\partial q_i}\ddot{q}_i \tag{10c}$$

$$\mathbf{A}_0 = \mathbf{I} \tag{10d}$$

$$\mathbf{B}_0 = \mathbf{C}_0 = \mathbf{0} \tag{10e}$$

where q is the joint angle and $\mathbf{T}_i$ is the link transformation matrix. The gradients of transformation matrices with respect to joint angles, joint angle velocities, and joint angle accelerations are

$$\frac{\partial \mathbf{A}_i}{\partial q_k} = \begin{cases} \mathbf{A}_{i-1}\dfrac{\partial \mathbf{T}_i}{\partial q_k} & (k=i) \\ \dfrac{\partial \mathbf{A}_{i-1}}{\partial q_k}\mathbf{T}_i & (k<i) \end{cases} \tag{11a}$$

$$\frac{\partial \mathbf{B}_i}{\partial q_k} = \begin{cases} \mathbf{B}_{i-1}\dfrac{\partial \mathbf{T}_i}{\partial q_k} + \mathbf{A}_{n-1}\dfrac{\partial^2 \mathbf{T}_i}{\partial q_k^2}\dot{q}_i & (k=i) \\ \dfrac{\partial \mathbf{B}_{i-1}}{\partial q_k}\mathbf{T}_i + \dfrac{\partial \mathbf{A}_{i-1}}{\partial q_k}\dfrac{\partial \mathbf{T}_i}{\partial q_i}\dot{q}_i & (k<i) \end{cases} \tag{11b}$$

$$\frac{\partial \mathbf{B}_i}{\partial \dot{q}_k} = \begin{cases} \mathbf{A}_{i-1}\dfrac{\partial \mathbf{T}_i}{\partial q_k} & (k=i) \\ \dfrac{\partial \mathbf{B}_{i-1}}{\partial \dot{q}_k}\mathbf{T}_i & (k<i) \end{cases} \tag{11c}$$

$$\frac{\partial \mathbf{C}_i}{\partial q_k} = \begin{cases} \mathbf{C}_{i-1}\dfrac{\partial \mathbf{T}_i}{\partial q_k} + 2\mathbf{B}_{i-1}\dfrac{\partial^2 \mathbf{T}_i}{\partial q_k^2}\dot{q}_i + \mathbf{A}_{i-1}\dfrac{\partial^3 \mathbf{T}_i}{\partial q_k^3}\dot{q}_i^2 \\ \quad + \mathbf{A}_{i-1}\dfrac{\partial^2 \mathbf{T}_i}{\partial q_k^2}\ddot{q}_i & (k=i) \\ \dfrac{\partial \mathbf{C}_{i-1}}{\partial q_k}\mathbf{T}_i + 2\dfrac{\partial \mathbf{B}_{i-1}}{\partial q_k}\dfrac{\partial \mathbf{T}_i}{\partial q_i}\dot{q}_i + \dfrac{\partial \mathbf{A}_{i-1}}{\partial q_k}\dfrac{\partial^2 \mathbf{T}_i}{\partial q_i^2}\dot{q}_i^2 \\ \quad + \dfrac{\partial \mathbf{A}_{i-1}}{\partial q_k}\dfrac{\partial \mathbf{T}_i}{\partial q_i}\ddot{q}_i & (k<i) \end{cases} \tag{11d}$$

$$\frac{\partial \mathbf{C}_i}{\partial \dot{q}_k} = \begin{cases} 2\mathbf{B}_{i-1}\dfrac{\partial \mathbf{T}_i}{\partial q_k} + 2\mathbf{A}_{i-1}\dfrac{\partial^2 \mathbf{T}_i}{\partial q_k^2}\dot{q}_i & (k=i) \\ \dfrac{\partial \mathbf{C}_{i-1}}{\partial \dot{q}_k}\mathbf{T}_i + 2\dfrac{\partial \mathbf{B}_{i-1}}{\partial \dot{q}_k}\dfrac{\partial \mathbf{T}_i}{\partial q_i}\dot{q}_i & (k<i) \end{cases} \tag{11e}$$

$$\frac{\partial \mathbf{C}_i}{\partial \ddot{q}_k} = \begin{cases} \mathbf{A}_{i-1}\dfrac{\partial \mathbf{T}_i}{\partial q_k} & (k=i) \\ \dfrac{\partial \mathbf{C}_{i-1}}{\partial \ddot{q}_k}\mathbf{T}_i & (k<i) \end{cases} \tag{11f}$$

DYNAMIC EQUATIONS OF MOTION

Dynamic equations of motion are important constraints in the optimization-based predictive dynamics problem of human running. The biggest challenge is the number of calculations to be performed because there are many matrix multiplications and additions for kinematics analysis. Also, the optimization process can take several iterations. These issues will be discussed in this section. Uicker (1965) derived the standard formulation for manipulator dynamics based on Lagrangian dynamics using DH 4×4 matrix transformations. However, that formulation takes order n^4 calculations. In 1979, Waters noticed that a simpler formulation can be derived that takes only order n^2 calculations. After that, Hollerbach (1980) derived a recursive formulation from the Waters formula that takes only order n calculations. Since we are solving an optimization problem, the number of multiplications and additions that need to be performed are significant.

RECURSIVE LAGRANGE DYNAMICS FORMULATION

The Lagrange's equation is given as

$$\tau_i = \frac{d}{dt}\left(\frac{\partial L}{\partial \dot{q}_i}\right) - \frac{\partial L}{\partial q_i} \tag{12}$$

where $L = K - V$ (kinetic energy – potential energy), q is the generalized coordinate vector (joint angles), and τ_i is joint torque vector. If any non-conservative force exists, it goes to the left side of Eq. (12). When $\mathbf{f}$ and $\mathbf{h}$ are conservative external global force and moment vectors acting on the linkage, respectively, Eq. (12) can be transformed to a recursive form given as

$$\mathbf{D}_i = \mathbf{J}_i \ddot{\mathbf{A}}_i^T + \mathbf{T}_{i+1}\mathbf{D}_{i+1} \tag{13a}$$

$$\mathbf{E}_i = m_i {}^i\mathbf{r}_i + \mathbf{T}_{i+1}\mathbf{E}_{i+1} \tag{13b}$$

$$\mathbf{F}_i = {}^k\mathbf{r}_f \delta_{ik} + \mathbf{T}_{i+1}\mathbf{F}_{i+1} \tag{13c}$$

$$\mathbf{G}_i = \mathbf{h}_k \delta_{ik} + \mathbf{G}_{i+1} \tag{13d}$$

$$\tau_i = tr\left[\frac{\partial \mathbf{A}_i}{\partial q_i}\mathbf{D}_i\right] + \mathbf{g}^T \frac{\partial \mathbf{A}_i}{\partial q_i}\mathbf{E}_i + \mathbf{f}_k^T \frac{\partial \mathbf{A}_i}{\partial q_i}\mathbf{F}_i + \mathbf{G}_i^T \mathbf{A}_{i-1}\mathbf{z}_0 \tag{13e}$$

$$\mathbf{D}_{n+1} = \mathbf{E}_{n+1} = \mathbf{F}_{n+1} = \mathbf{G}_{n+1} = \mathbf{0} \tag{13f}$$

where $\mathbf{J}_i$ is the inertia matrix for link i, $\mathbf{g}$ is gravity vector, ${}^i\mathbf{r}_i$ is the location of the center of mass in the i^{th} local frame, ${}^k\mathbf{r}_f$ is the location of the external force acting in the k^{th} frame, $\mathbf{z}_0 = [0\ 0\ 1\ 0]^T$, and δ_{ik} is Kronecker delta. The segment masses in the mechanical model are calculated using a mass distribution formula (Chaffin and Andersson, 1984). The link length and joint locations are determined based on high resolution 3D scanned data (Eyetronics). All the segments are assumed as slender bars, and the mass moments of inertia are calculated under this assumption.

The derivatives of equations of motion with respect to joint angles, joint angle velocities, and joint angle accelerations are

$$\frac{\partial \tau_i}{\partial q_k} = \begin{cases} tr\left(\dfrac{\partial^2 \mathbf{A}_i}{\partial q_i \partial q_k}\mathbf{D}_i + \dfrac{\partial \mathbf{A}_i}{\partial q_i}\dfrac{\partial \mathbf{D}_i}{\partial q_k}\right) + \mathbf{g}^T \dfrac{\partial^2 \mathbf{A}_i}{\partial q_i \partial q_k}\mathbf{E}_i \\ \qquad + \mathbf{f}^T \dfrac{\partial^2 \mathbf{A}_i}{\partial q_i \partial q_k}\mathbf{F}_i + \mathbf{G}_i^T \dfrac{\partial \mathbf{A}_{i-1}}{\partial q_k}\mathbf{z}_0 & (k \le i) \\ tr\left(\dfrac{\partial \mathbf{A}_i}{\partial q_i}\dfrac{\partial \mathbf{D}_i}{\partial q_k}\right) + \mathbf{g}^T \dfrac{\partial \mathbf{A}_i}{\partial q_i}\dfrac{\partial \mathbf{E}_i}{\partial q_k} + \mathbf{f}^T \dfrac{\partial \mathbf{A}_i}{\partial q_i}\dfrac{\partial \mathbf{F}_i}{\partial q_k} & (k > i) \end{cases} \tag{14a}$$

$$\frac{\partial \tau_i}{\partial \dot{q}_k} = tr\left(\frac{\partial \mathbf{A}_i}{\partial q_i}\frac{\partial \mathbf{D}_i}{\partial \dot{q}_k}\right) \tag{14b}$$

$$\frac{\partial \tau_i}{\partial \ddot{q}_k} = tr\left(\frac{\partial \mathbf{A}_i}{\partial q_i}\frac{\partial \mathbf{D}_i}{\partial \ddot{q}_k}\right) \tag{14c}$$

COMPUTATIONAL CONSIDERATION

The number of multiplications and additions for each formulation are summarized in Table 1. The order of calculations for the three formulations noted previously can be observed in the table. For a system with small DOF, the total computational time with the three formulations may not be too different. However, for a model with a large number of DOF (such as the Santos model with 55 DOF), the number of calculations can be significantly different. This can have a significant impact on the efficiency of the entire optimization process. It is clear that the recursive formulation is the most suitable for digital human modeling, and it is used for the running problem.

Table 1 Number of multiplication and additions (*n*: number of transformation matrices)

Method	Multiplications	Additions
Uicker (1965)	32 1/2 n^4+86 5/12 n^3 +171 1/4 n^2 + 5 1/3 n -128	25 n^4 + 66 1/3 n^3 +129 1/2 n^2 +42 1/3 n -96
Waters (1979)	106 1/2 n^2 + 620 1/2 n – 512	82 n^2 + 514 n – 384
Hollerbach (1980)	830 n - 592	675 n - 464

Table 2 Number of multiplications and additions for *n*=55

Method	Multiplications	Additions	Total
Uicker (1965)	312293722	240195803	552489525
Waters (1979)	355778	275936	631714
Hollerbach (1980)	45058	36661	81719

VERIFICATION OF EQUATIONS OF MOTION

The equations of motion were verified by the forward dynamics process using a commercial general-purpose multi-body dynamics software code (ADAMS). The single pendulum problem was solved for this process.

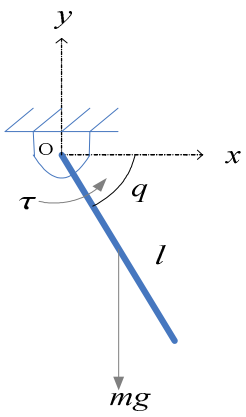

Figure 6 Single pendulum

Figure 6 depicts the single pendulum model in which mass is 0.5 kg, length is 0.4 m, and it is assumed to be a slender bar. The equation of motion is given by

$$I\ddot{q} + mg\frac{l}{2}\cos q = \tau \tag{15}$$

The initial position is q= 0, and the ADAMS results are shown in Figure 7.

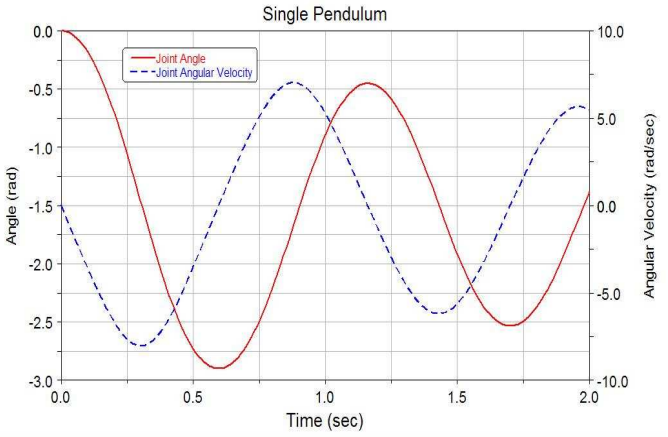

Figure 7 Join angle and joint angle velocity of single pendulum

Since it is a free vibrations problem, there should not be non-conservative joint torque (τ = 0). By using ADAMS, the joint torque is indeed obtained as zero, thus verifying the current equations of motion formulation.

STABILITY

ZERO MOMENT POINT

Another important consideration for the running problem is the dynamic stability of the motion. The most common constraint to achieve stability for biped gait analysis is the zero moment point (ZMP) constraint in the support phase. Zero moment point can be derived by using the following steps.

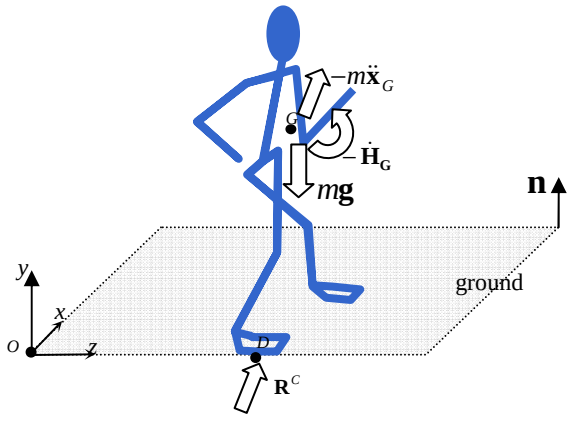

Figure 8 Description of ZMP

In Figure 8, point D is ZMP, which needs to be determined. The resultant moment about the ZMP by inertia, gravity, and external force (IGF) is given as

$$\mathbf{M}_D^{IGF} = \mathbf{x}_{DG} \times m\mathbf{g} - \mathbf{x}_{DG} \times m\ddot{\mathbf{x}}_G - \dot{\mathbf{H}}_G \tag{16}$$

where $\dot{\mathbf{H}}_G$ is rate of angular momentum about the center of mass of the system. The resultant moment about the point O is

$$\mathbf{M}_O^{IGF} = \mathbf{x}_{OG} \times m\mathbf{g}_G - \mathbf{x}_{OG} \times m\ddot{\mathbf{x}}_G - \dot{\mathbf{H}}_G \tag{17}$$

Then Eq. (17) can be written as

$$\mathbf{M}_D^{IGF} = \mathbf{M}_O^{IGF} - \mathbf{x}_{OD} \times \mathbf{R}^{IGF} \tag{18}$$

From the condition that the tripping moment by the IGF measured at the D is zero, we have

$$\begin{aligned} \mathbf{n} \times \mathbf{M}_D^{IGF} &= \mathbf{n} \times \mathbf{M}_O^{IGF} - \mathbf{n} \times (\mathbf{x}_{OD} \times \mathbf{R}^{IGF}) \\ &= \mathbf{n} \times \mathbf{M}_O^{IGF} - (\mathbf{n} \cdot \mathbf{R}^{IGF})\mathbf{OD} + (\mathbf{n} \cdot \mathbf{x}_{OD})\mathbf{R}^{IGF} \\ &= \mathbf{0} \end{aligned} \tag{19}$$

where $\mathbf{n}$ is a unit vector that is normal to ground plane. Then, the ZMP location is obtained as

$$\mathbf{x}_{OD} = \frac{\mathbf{n} \times \mathbf{M}_O^{IGF}}{\mathbf{n} \cdot \mathbf{R}^{IGF}} \tag{20}$$

ZERO YAWING MOMENT

The zero yawing moment (ZYM) constraint is usually imposed for the upper-body motion to be compensated by the lower-body motion. From Eq. (16), the yawing moment about the ZMP D is obtained as

$$\begin{aligned} Y_D^{IGF} &= \mathbf{M}_D^{IGF} \cdot \mathbf{n} \\ &= \sum_i^{n_{body}} \left[\mathbf{x}_{DG_i} \times (m_i\mathbf{g} - m_i\ddot{\mathbf{x}}_{G_i}) - \dot{\mathbf{H}}_{G_i} \right] \cdot \mathbf{n} \\ &= \sum_i^{n_{body}} \left[\mathbf{x}_{DG_i} \times (m_i\mathbf{g} - m_i\ddot{\mathbf{x}}_{G_i}) \right] \cdot \mathbf{n} \end{aligned} \tag{21}$$

where $\dot{\mathbf{H}}_{G_i}$ is assumed to be zero.

FORMULATION

The problem is to determine the joint angle profiles that minimize an energy cost function. It is assumed that the running motion is completely periodic and symmetric and that there are two phases, support and flight. To solve this optimization problem, a skeletal model of the human and the running speed are needed as input. Through the optimization process, joint angle profile, joint torque profile, and contact force profile are obtained as output, as shown in Figure 9.

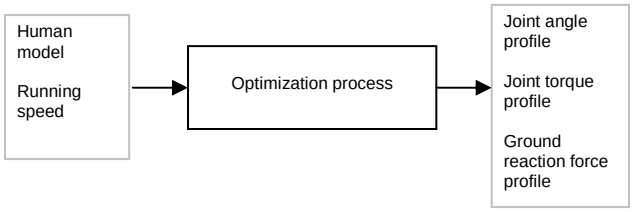

Figure 9 Input and output of running problem

Design variables are

$$DV : \mathbf{q} \tag{22}$$

where $\mathbf{q}$ is joint angle profiles. The cost function is

$$f = \int_0^t \boldsymbol{\tau}^T \boldsymbol{\tau} dt \tag{23}$$

which is the proportional to the mechanical energy. This mechanical energy is a reasonable criterion to minimize (Roussel et al. 1998).

CONSTRAINTS

Most constraints are motivated by the digital human walking formulation (Xiang et al. 2007). The constraints are listed as follows:

1. Joint limits
2. Ground penetration
3. Foot location of ground contact point
4. Impact constraint (zero velocity at foot strike)
5. ZMP during support phase
6. ZYM
7. Symmetry condition

Current joint angle limits for the body are determined based on Norkin and White (2003).

Impact constraint (zero velocity at foot strike)

As we know, there is a flight phase in human running. At the end of this flight phase, there is impact. In this impact, there is the sudden change of joint angle velocities. Therefore, this sudden change of joint angle velocities results in an impulsive force at the foot impact. To handle the impact stage in the current implementation, we set the heel velocity to zero when the foot strike occurs.

$$\dot{\mathbf{x}}_i(t) = 0, \qquad 0 \le t \le T, \qquad i \in contact \tag{24}$$

ZMP constraint

To implement the zero moment point constraint in the current formulation, we consider the x-z plane as the ground in Figure 6. In other words, the normal vector $\mathbf{n}$ is $[0, 1, 0]^T$. In this case, we can simplify the ZMP calculation from Eq. (20) as

$$z_{zmp} = \frac{\sum_i^n m_i(\ddot{y}_i + g) z_i - m_i \ddot{z}_i y_i + J_i \ddot{q}_{ix}}{\sum_i^n m_i(\ddot{y}_i + g)} \tag{25a}$$

$$x_{zmp} = \frac{\sum_i^n m_i(\ddot{y}_i + g) x_i - m_i \ddot{x}_i y_i + J_i \ddot{q}_{iz}}{\sum_i^n m_i(\ddot{y}_i + g)} \tag{25b}$$

Here, the zero moment point is simply a point where the moments about the x and z axes due to IGF are zero.

Zero yawing moment constraint

The yawing moment constraint is imposed as

$$\left| Y_D^{IGF} \right| \le Y_D^U \tag{26}$$

where Y_D^{IGF} is the resultant yawing moment about the y axis and Y_D^U is an upper bound for it. In the current implementation, Y_D^U is set to zero. From Eq. (21), the zero yawing moment constraint is simplified with $\mathbf{n}$ = [0, 1, 0]^T as

$$Y_D^{IGF} = \sum_i^{n_{body}} m_i \left[\left(z_i - z_{zmp} \right) \ddot{x}_i - \left(x_i - x_{zmp} \right) \ddot{z}_i \right] \tag{27}$$

STEP LENGTH AND FLIGHT TIME

The step length and flight time were formulated as a function of running speed and running frequency, respectively (Bruderlin and Calvert, 1996). The step length sl is given as

$$sl = 0.1394 + (0.00465 + level) v \sqrt{\frac{body\_height}{1.8}} \tag{28}$$

where v is running speed (m/min), $level$ is the level of expertise in running (–0.001 as poor ≤ $level$ ≤ 0.001 as skilled), $body\_height$ is the height of the human body. The flight time t_{flight} is given as

$$t_{flight} = -0.675 \times 10^{-3} - (0.15 \times 10^{-3} + level) sf + 0.542 \times 10^{-5} sf^2 \tag{29a}$$

$$t_{flight} = -8.925 + (0.131 + level) sf - 0.623 \times 10^{-3} sf^2 + 0.979 \times 10^{-6} sf^3 \tag{29b}$$

where sf is step frequency (steps/min, $sf = v / sl$). Eq. (29a) is used when sf is 0~180 steps/min, and Eq. (29b) is used when sf is 180~230 steps/min.

RESULTS

To evaluate the formulation, models with and without arms were used. The model without arms has 26 DOF (6 global DOF, 7 DOF for each leg, and 6 DOF for spine). Figure 10(a) depicts joints in the model without arms, and Figure 10(b) depicts joints in the full-body model (55 DOF).

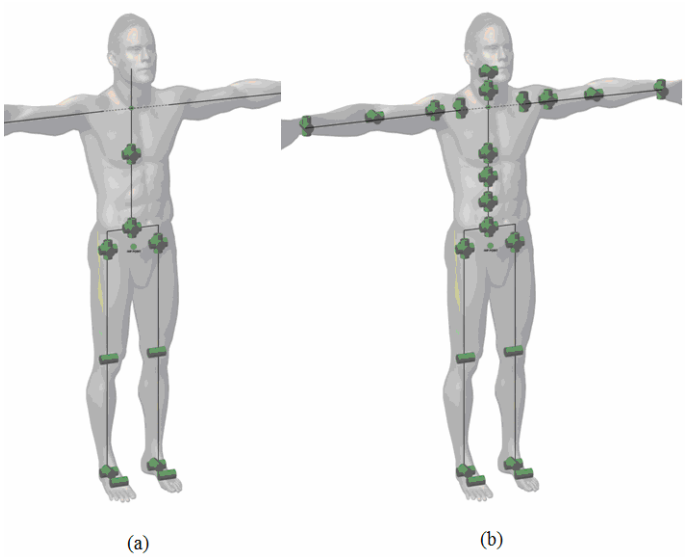

Figure 10 (a) Model without arms (b) Full-body model

The number of control points is taken as 5 for each DOF. Thus, the total number of design variables is 130 for the model without arms and 275 for full-body model. An Intel Pentium 3.46 GHz CPU PC was used to obtain the optimum solutions.

Figure 11 is a snapshot of Santos™ running at a speed of 2 m/s. The step length is 0.8 m, and the model without the arms was used for this simulation.

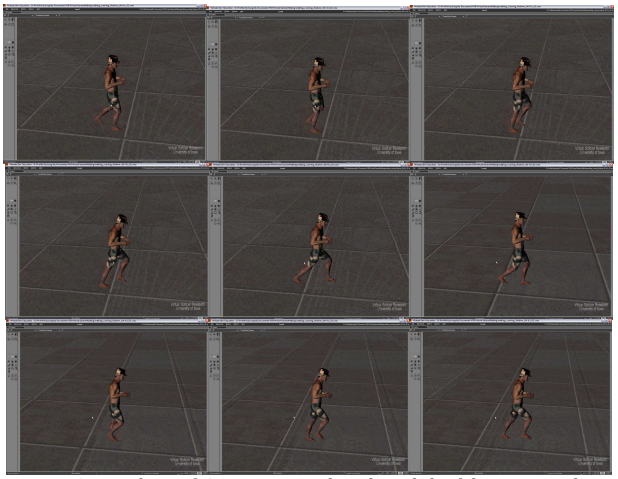

Figure 11 Snapshot of Santos running (model without arms)

Figure 12 is a snapshot for the case where a backpack is included. The model without arms was used for this case as well. The running speed was 1.8 m/s and step length was 0.6 m. The backpack mass was 10.20 kg (100 N).

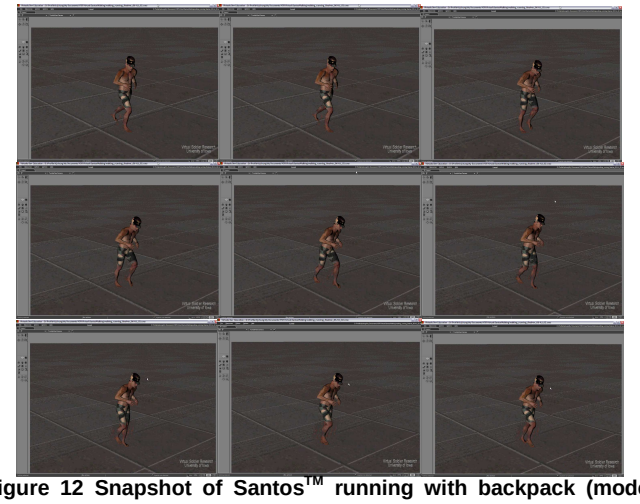

Figure 12 Snapshot of Santos™ running with backpack (model without arms)

Figure 13 is a snapshot of Santos running with the full-body model. In this simulation, the initial and end points were specified for the elbow as additional constraints.

Figure 13 Snapshot of Santos running with arm motion

Figure 14 is a comparison of the joint angles for the spine between normal running and running with backpack (Figures 11 and 12).

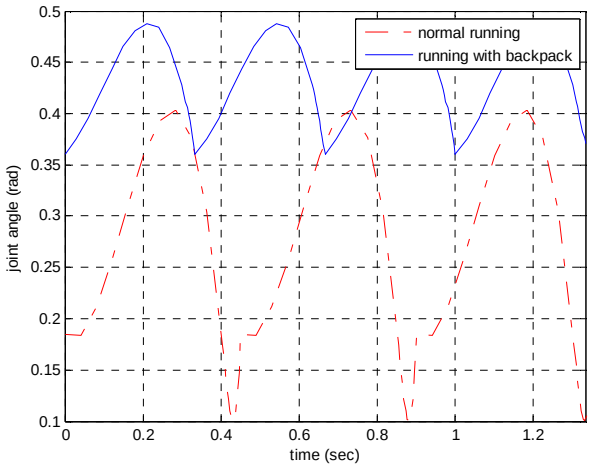

Figure 14 Comparison of spine joint angles

Figure 15 and Figure 16 are a right knee joint angle profile and a ground reaction force profile respectively for the full-body model.

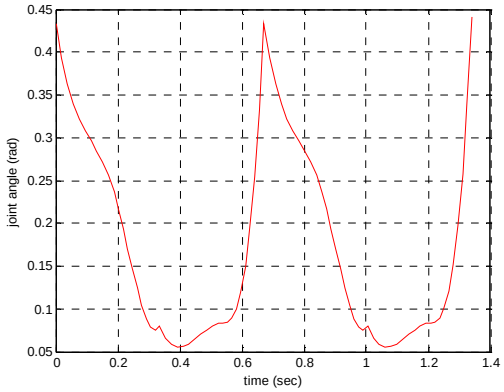

Figure 15 Right knee joint angle profile

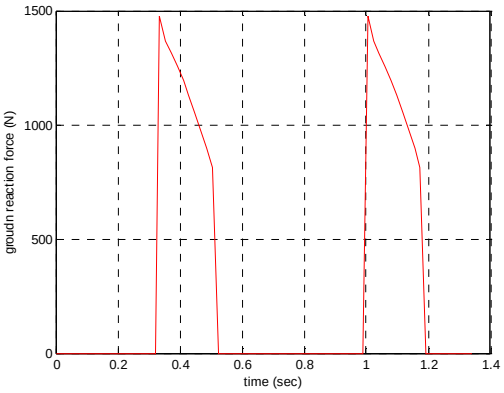

Figure 16 Ground reaction force on right foot

The simulation results are compared those from the experiments (Patla et al. 1989, Ounpuu 1994). The two results do not match exactly since the dimension and mass properties of the experimental subjects are different from those for the mechanical model. However, the trend are similar to the simulation results. For the ground reaction force, shape of the impact moment is a little different from the experimental data. These aspects need to be investigated further to refine the formulation of the problem.

CONCLUSION

The task of digital human running was formulated as an optimization problem. Using the optimization process, it is possible to predict dynamic motion (joint angle profiles) as well as the corresponding joint torques. A predictive dynamics approach was used where there was no need to integrate the equations of motion, as with the forward dynamics formulation. B-spline interpolation was used for discretization along the time axis, and the Denavit-Hartenberg method was used for kinematics analysis of the mechanical system. For dynamic equilibrium, the recursive Lagrange method was used to reduce the order of computations. For dynamic stability, zero moment point and zero yawing moment constraints were used. To formulate the impact stage, the zero velocity at foot strike was used. The mechanical structure of Santos^{TM} was developed with (1) a model without arms, which had 26 DOF, and (2) a full-body model, which had 55 DOF. As a separate case, an external load was applied as a backpack. With the full-body model, we could observe the upper-body motion, especially the arm motion. The step length and flight time were given as a functions of running speed and running frequency, respectively. A more detailed validation of the formulation for the running problem is in progress that will be reported later.

ACKNOWLEDGMENTS

This research is funded by Natick's Biomechanical Simulator System (BAS) (Contract Number: W911WY-06-C-0034).

REFERENCES

1. Bruderlin, A. and Calvert, T. 1996. "Knowledge-driven, interactive animation of human running." *Proceedings of the Conference on Graphics Interface*, 213-221.
2. Cavanagh, P. and Lafortune, M. 1980. "Ground reaction forces in distance running." *Journal of Biomechanics*, 13, 397-406.
3. Chaffin, D. B. and Andersson, G. B. J. 1984. *Occupational Biomechanics*. New York: John Wiley & Sons, Inc.
4. Chevallereau, C. and Aoustin, Y. 2001. "Optimal reference trajectories for walking and running of a biped robot." *Robotica*, 19, 557-569.
5. Denavit, J. and Hartenberg, R. S. 1955. "A kinematic notation for lower-pair mechanisms based on matrices." *ASME Journal of Applied Mechanics*, 22, 215–221.
6. Dillman, C. 1975. "Kinematic analysis of running." *Exercise and Sport Sciences Reviews 3*, 193-218.
7. Eyetronics."Bodybuilder."<http://www.eyetronics.com/digitalhumans/digitalhumans/digitalhumans/digitalhumans_detail.php?type=body&id=3>
8. François, C. and Samson, C. 1994. "Running with constant energy." *IEEE International Conference on Robotics and Automation*, 1, 131-136.
9. Fujimoto, Y. 2004. "Minimum energy biped running gait and development of energy regeneration leg." *The 8th IEEE International Workshop on Advanced Motion Control*, 415-420.
10. Gienger, M., Löffler, K., and Pfeiffer, F. 2000. "A biped robot that jogs." *IEEE International Conference on Robotics and Automation* (April).
11. Hamill, J., Derrick, T.R. and Holt, K.G. 1995. "Shock attenuation and stride frequency during running." *Human Movement Science*, vol. 14, 45-60.
12. Hardin, E.C., Van Den Bogert, A.J. and Hamill, J. 2004. "Kinematic adaptations during running: effects of footwear, surface, and duration." *Medicine and Science in Sports and Exercise*, 36(5), 838-844.

13. Hirai, K., Hirose, M., Haikawa, Y., and Takenaka, T. 1998. “The development of Honda humanoid robot.” *IEEE international Conference on Robotics and Automation*.
14. Hodgins, J., and Raibert, M. 1991. “Adjusting step length for rough terrain locomotion.” *IEEE Transactions on Robotics and Automation*, 7(3), 289-298
15. Hodgins, J. 1996. “Three-dimensional human running.” *International Conference on Robotics and Automation*.
16. Högberg, P. 1952. “Length of stride, stride frequency, ‘flight’ period and maximum distance between the feet during running with different speed.” *Arbeitsphysiologie*, *14*, 431-436.
17. Hollerbach, J. 1980. “A recursive Lagrangian formulation of manipulator dynamics and a comparative study of dynamics formulation complexity.” *IEEE Trans. Systems, Man, and Cybernetics*, 10, 730-736.
18. Honda ASIMO world wide website. <http://asimo.honda.com/default.aspx>
19. Kang, Y., Cho, H., and Lee, E. 1999. “An efficient control over human running animation with extension of planar hopper model.” *The Journal of Visualization and Computer Animation*, 10, 215-224.
20. Kawamura, A., Sugio, K., Suzuki, K., and Zhu, C. 2004. “Simulation study on one leg jumping for biped running.” *The 8th IEEE International Workshop on Advanced Motion Control*, 433-438.
21. Kim, H., Horn, E., Xiang, Y., Abdel-Malek, K., and Arora, J. 2004. “Digital human modeling and virtual reality for FCS: Dynamic motion prediction of gait and lifting.” Technical Report, Virtual Soldier Research Lab, The University of Iowa.
22. Nagasaki, T., Kajita, S., Yokoi, K., Kaneko, K. and Tanie, K. 2003. “Running pattern generation and its evaluation using a realistic humanoid model.” *Proceedings of the IEEE International Conference on Robotics and Automation*, 1, 1336-1342.
23. Norkin, C. C. and White, D. J. 2003. *Measurement of Joint Motion: A Guide to Goniometry, 3rd Edition.* Philadelphia: F. A. Davis Co.
24. Novacheck, T. 1998. “The biomechanics of running.” *Gait and Posture*, 7, 77-95
25. Ounpuu, S. 1994. “The biomechanics of walking and running.” *Clinics in Sports Medicine*, 13(4), 843-863.
26. Park, J. and Kwon, O. 2003. “Impedance control for running of biped robots.” *Proceedings of the IEEE/ASME International Conference on Advanced Intelligent Mechatronics*, 2, 944-949.
27. Patla, A. E., Robinson, C., Samways, M. and Armstrong, C. J. 1989. “Visual control of step length during overground locomotion: Task-specific modulation of the locomotor synergy.” *Journal of Experimental Psychology*, 15 (3), 603-617.
28. Roussel, L., Canuda-de-Wit, C. and Goswami, A. 1998. “Generation of energy optimal complete gait cycles for biped robots.” *Proceedings of the IEEE International Conference on Robotics and Automation*, 3, 2036-2041
29. Simpson, K. and Bates, B. 1990. “The effects of running speed on lower extremity joint moments generated during the support phase.” *International Journal of Sport Biomechanics*, 6, 309-324.
30. Uicker, J. J. 1965. “On the dynamic analysis of spatial linkages using 4 × 4 matrices.” *Ph.D. Dissertation, Northwestern University.*
31. Vukobratović, M., Borovac, B., Surla, D. and Stokić, D. 1990. Scientific Fundamentals of Robots7: Biped Locomotion – Dynamics, Stability, Control and Application. Springer-Verlag
32. Vukobratović, M. and Borovac, B. 2004. “Zero-moment point – thirty five years of its life.” *International Journal of Humanoid Robotics*, 1(1), 157-173.
33. Waters, R. C. 1979. “Mechanical arm control.” *M.I.T. Artivicial Intelligence Lab. Memo*. 549.
34. Westervelt, E. R. and Grizzle, J. W. 2003. “Hybrid zero dynamics of planar biped walkers.” *The University of Pennsylvania, Department of Electrical and Systems Engineering, Departmental Paper*.
35. Xiang, Y., Chung, H. J., Mathai, A., Rahmatalla, S., Kim, J., Marler, T., Beck, S., Yang, J., Arora, J. S. and Abdel-Malek, K. 2007. “Optimization-based dynamic human walking prediction.” *Proceedings of the Digital Human Modeling Conference*.

CONTACT

Corresponding author: J.S. Arora. Email: jasbir-arora@uiowa.edu; telephone: (319) 335-5658; fax: (319) 335-5660